Supplementary Information (SI)

Low-temperature Atomic Layer Deposition of Metastable MnTe Films for Phase Change Memory

Gwangsik Jeon[a], Jeongwoo Jeon[a], Woohyun Kim[a], Daehyeon Kim[b], Wontae Noh[b], Wonho Choi[a], Byongwoo Park[a], Sangmin Jeon[a], Sungjin Kim[a], Chanyoung Yoo[c], and Cheol Seong Hwang*[a]*

[a]Department of Materials Science and Engineering and Inter-University Semiconductor Research Center, Seoul National University, Seoul, 08826, Republic of Korea

[b]Air Liquide Korea Co., LTD., Seoul, 03722, Republic of Korea

[c]Department of Materials Science and Engineering, Hongik University, Seoul, 04066, Republic of Korea

**Corresponding author (e-mail: cyyoo@hongik.ac.kr, cheolsh@snu.ac.kr)*

Table S1. Properties of various common Mn precursors.

Precursor	$Mn(N(SiMe_3)_2)_2$ (This work)	$Mn(EtCp)_2$	$Mn(MeCp)_2$	$Mn_2(CO)_{10}$	$Mn(thd)_3$
Oxidation state	+2	+2	+2	0	+3
Melting point (°C)	~58	Liquid at R. T.	~69	~154	~165
Vapor pressure	1 torr @ 78 °C	0.1 torr @ 50-65 °C	1 torr @ 85-90 °C	0.5 torr @ 60 °C	No data
Properties	Flammable	Flammable	Flammable	Flammable	Irritant
Remarks	Mn-N bonds	Mn-C bonds	Mn-C bonds	Mn-C bonds	Mn-O bonds
Ref	Not reported	Oxide (100 ~ 300 °C)[1–3] Sulfide (100 ~ 225 °C)[4]	MnAs (320 ~ 500 °C)[5]	Oxide (80~160 °C)[6]	Oxide (140~300 °C)[7–10]

Table S2. Enthalpy and Gibbs free energy change from DFT calculation.

Entry	Reaction (T = 100 °C)	ΔH ($kJ \cdot mol^{-1}$)	ΔG ($kJ \cdot mol^{-1}$)
(i)	$(Me_3Si)_2Te + 2NH_3 \rightarrow H_2Te + 2Me_3SiNH_2$	-28.63	-39.19
(ii)	$Mn(N(SiMe_3)_2)_2 + NH_3 \rightarrow H_2NMnN(SiMe_3)_2 + HN(SiMe_3)_2$	-85.60	-100.53
(iii)	$H_2NMnN(SiMe_3)_2 + H_2Te \rightarrow HTeMnN(SiMe_3)_2 + NH_3$	-63.90	-74.54

Table S3. Local atomic compositions of Mn and Te for the films deposited on 1:29 AR holes.

Location	Mn (at%)	Te (at%)
Top	47.93	52.07
Middle	49.80	50.20
Bottom	52.57	47.47

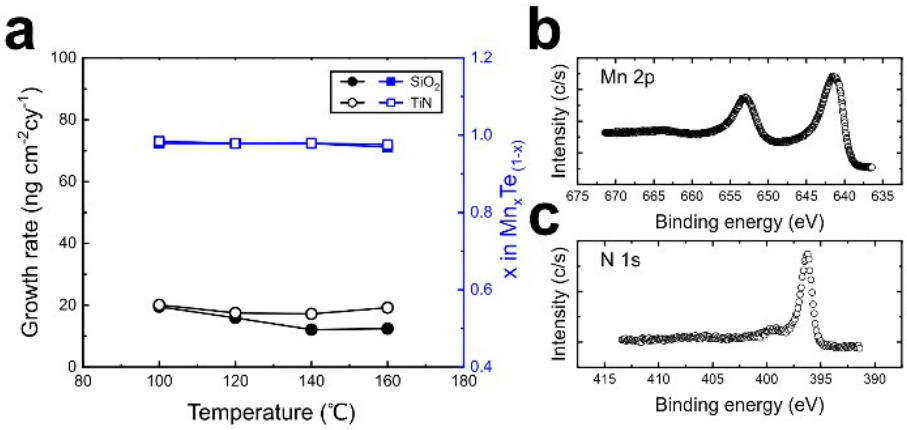

Figure S1. (a) Effect of substrate temperature when NH_3 was coinjected with Mn precursor, not Te precursor. (b) Mn 2p, (c) N 1s XPS spectra of the films grown by Mn precursor with NH_3 coinjection (Mn + NH_3 pulse/Ar purge).

Injecting NH_3 after the Mn precursor without coinjection with the Te precursor (Mn precursor/Ar purge/NH_3/Ar purge/Te precursor/Ar purge) did not deposit any film. Coinjecting NH_3 with the Mn precursor (Mn precursor + NH_3/Ar purge/Te precursor/Ar purge) led to Mn-rich (~90 %) films at all temperatures (Figure S1a). When coinjecting the Mn precursor and NH_3 in the absence of the Te precursor (Mn precursor + NH_3/purge), XPS analysis of the deposited film revealed the existence of Mn and N peaks (Figure S1b, c). This result indicates that NH_3 reacts with the $N(SiMe_3)$ ligand of the Mn precursor, converting it to highly reactive NH_2 groups. However, even with these reactive surface groups, the absence of NH_3 coinjection with BTMS-Te results in insufficient Mn-Te formation, leading to Mn-rich films. Thus, coinjecting NH_3 with Te precursor to generate reactive H_2Te is crucial for the optimized deposition.

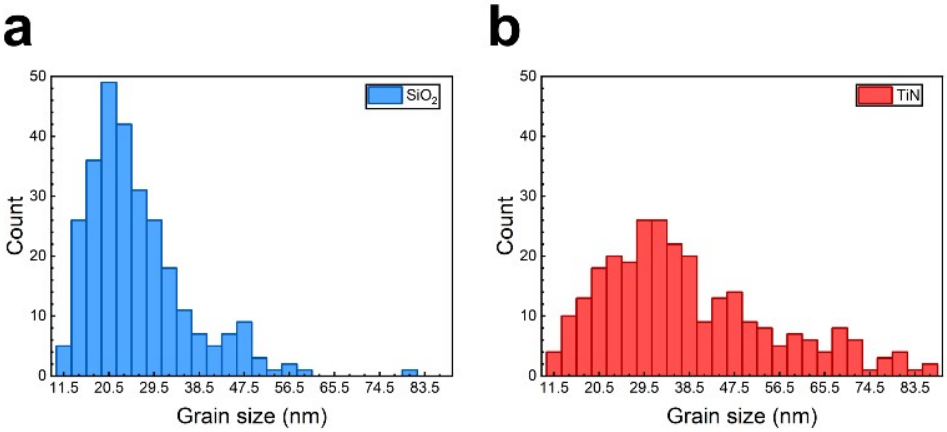

Figure S2. Grain size distribution of the MnTe films on (a) SiO_2 and (b) TiN substrates grown at 100 ℃.

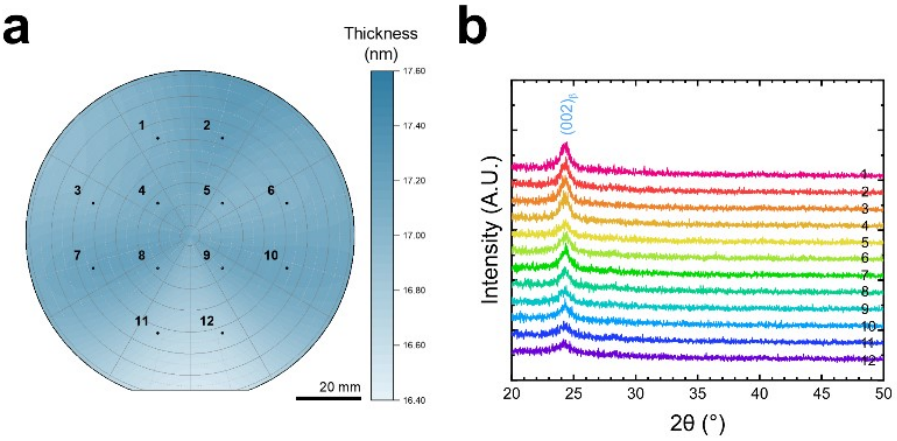

Figure S3. (a) Thickness mapping of a 17 nm-thick uniform MnTe film on a 4-inch SiO_2 substrate. (b) GAXRD results obtained at 12 different locations, indicated by the black dots and numbers.

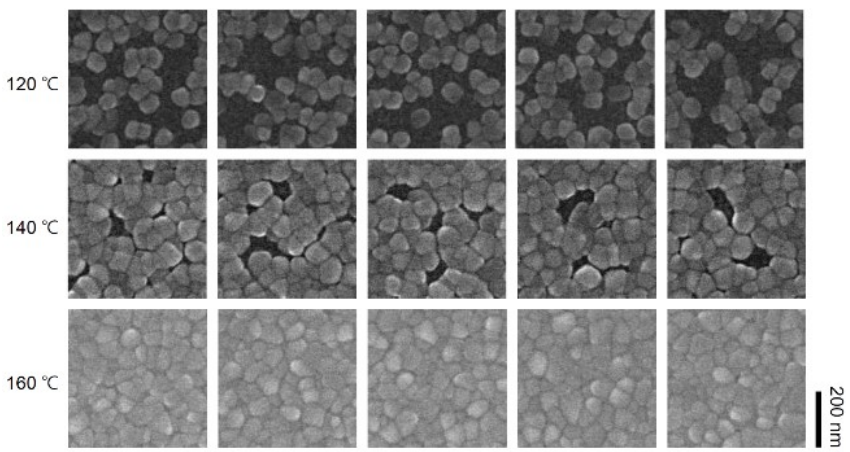

Figure S4. SEM images of MnTe films on SiO_2 used for calculating the density of grains at each temperature.

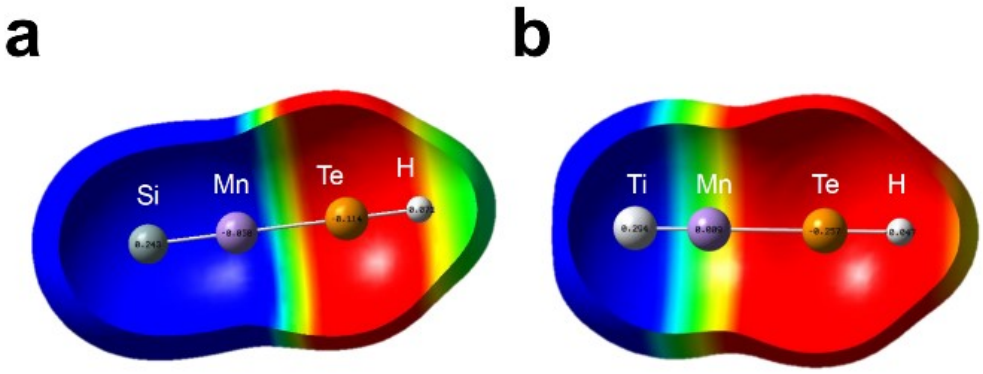

Figure S5. DFT simulations for comparison of electron density of MnTe bonded with (a) Si and (b) Ti. The relative charges are indicated on each atom.

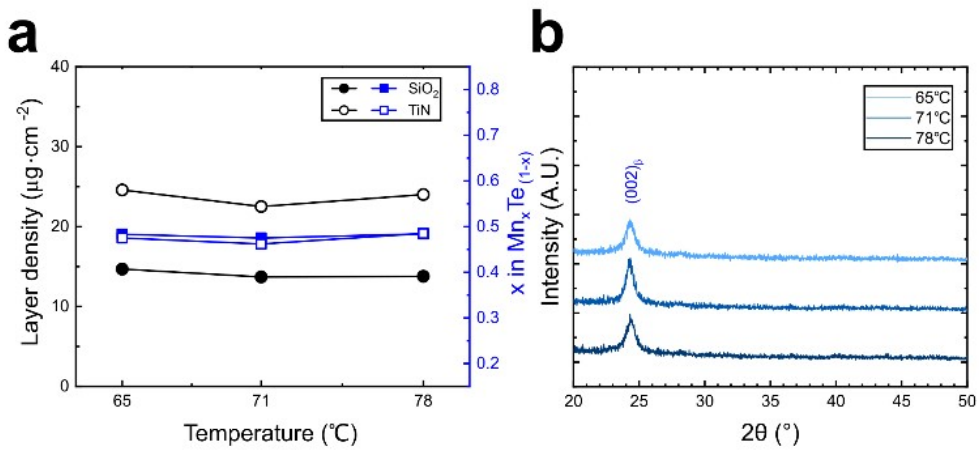

Figure S6. (a) Effect of the Mn canister temperature on the growth rate. (b) GAXRD results of MnTe films at various Mn canister temperatures on SiO_2 substrates.

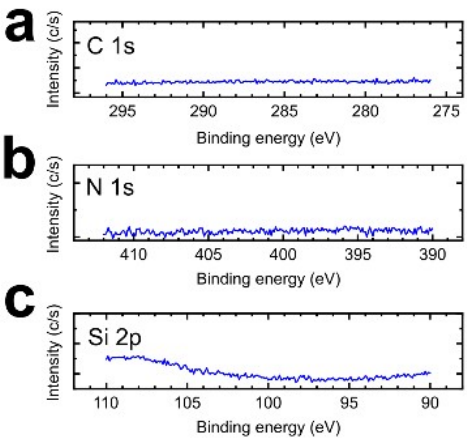

Figure S7. (a) C 1s, (b) N 1s, (c) Si 2p XPS spectra of the MnTe film on SiO_2 substrates grown at 100 ℃.

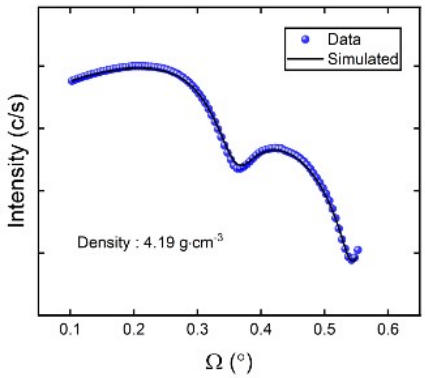

Figure S8. XRR results of the MnTe film on SiO_2 substrates grown at 100 ℃.

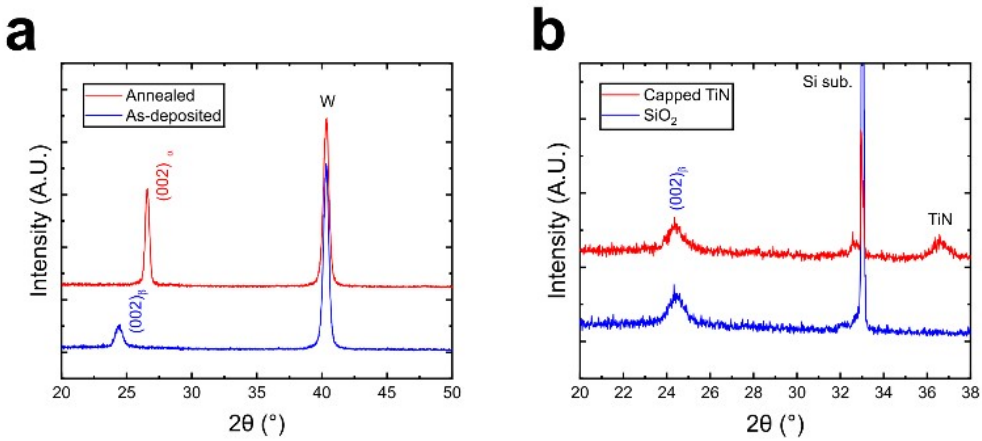

Figure S9. (a) GAXRD results of as-deposited and annealed MnTe films. (b) XRD results of MnTe films on SiO_2 and SiO_2 capped TiN grown at 100 ℃.

Note and references

1. B. B. Burton, F. H. Fabreguette and S. M. George, *Thin Solid Films*, 2009, **517**, 5658–5665.
2. M. J. Young, C. D. Hare, A. S. Cavanagh, C. B. Musgrave and S. M. George, *ACS Appl. Mater. Interfaces*, 2016, **8**, 18560–18569.
3. K. L. Pickrahn, Y. Gorlin, L. C. Seitz, A. Garg, D. Nordlund, T. F. Jaramillo and S. F. Bent, *Phys. Chem. Chem. Phys.*, 2015, **17**, 14003–14011.
4. S. C. Riha, A. A. Koegel, X. Meng, I. S. Kim, Y. Cao, M. J. Pellin, J. W. Elam and A. B. F. Martinson, *ACS Appl. Mater. Interfaces*, 2016, **8**, 2774–2780.
5. M. Ozeki, T. Haraguchi and A. Fujita, *J. Cryst. Growth*, 2007, **298**, 90–93.
6. H. Jin, D. Hagen and M. Karppinen, *Dalt. Trans.*, 2016, **45**, 18737–18741.
7. O. Nilsen, H. Fjellvåg and A. Kjekshus, *Thin Solid Films*, 2003, **444**, 44–51.
8. F. Mattelaer, P. M. Vereecken, J. Dendooven and C. Detavernier, *Chem. Mater.*, 2015, **27**, 3628–3635.
9. H. E. Nieminen, V. Miikkulainen, D. Settipani, L. Simonelli, P. Hönicke, C. Zech, Y. Kayser, B. Beckhoff, A. P. Honkanen, M. J. Heikkilä, K. Mizohata, K. Meinander, O. M. E. Ylivaara, S. Huotari and M. Ritala, *J. Phys. Chem. C*, 2019, **123**, 15802–15814.
10. V. Miikkulainen, A. Ruud, E. Østreng, O. Nilsen, M. Laitinen, T. Sajavaara and H. Fjellvaìšg, *J. Phys. Chem. C*, 2014, **118**, 1258–1268.